Electronic supplementary information (ESI) for:

One-pot facile synthesis of rod-like Bi2S3 particle in deep eutectic solvent and its ppb-level selective H2S gas detection

Reiko Furukawa,[a] Takuya Hasegawa,[a]* Ayahisa Okawa[a] and Shu Yin[a,b]

[a] *Institute of Multidisciplinary Research for Advanced Material (IMRAM), Tohoku University, 2-1-1 Katahira, Aoba-ku, Sendai, Miyagi, 980-8577, Japan*

[b] *Advanced Institute for Materials Research (WPI-AIMR), Tohoku University, 2-1-1 Katahira, Aoba-ku, Sendai, Miyagi, 980-8577, Japan*

†Corresponding author:
Dr. Takuya Hasegawa
Tel/Fax +81-22-217-5598, E-mail: hase@tohoku.ac.jp

Contents

METHODS

Materials. The chemicals used in the preparation of DESs and synthesis of the Bi_2S_3 included the following: thioacetamide (TAA, CH_3CSNH_2; >98.0 %), glycerol (Gly, $C_3H_5(OH)_3$; >99.0 %), urea (Ure, $CO(NH_2)_2$; >99.0 %), levulinic acid (Lev, $CH_3COCH_2CH_2CO_2H$; 98.0 %), acetamide (Act, CH_3CONH_2; >98.0 %), and choline chloride (ChCl, $[(CH_3)_3NCH_2CH_2OH]Cl$; >95.0 %), all sources were purchased from Wako Pure Chemical Industries. Bismuth nitrate pentahydrate ($Bi(NO_3)_3{\cdot}5H_2O$; >99.9 %) was obtained from Kanto Chemical Co., Inc. All compounds were utilized without further purification.

Materials synthesis. Bismuth sulfide, Bi_2S_3, was synthesized by a facile heating method with various DESs as the reaction solvent. The HBDs were prepared by mixing 1 mmol of TAA and 49 mmol of different types of HBDs: glycerol, urea, levulinic acid, and acetamide. The DESs were prepared by mixing 25 mmol of ChCl as the HBA and 50 mmol of each mixed HBD, heating the mixture at 70 °C until a homogeneous liquid phase was achieved. Subsequently, 0.5 mmol of $Bi(NO_3)_3{\cdot}5H_2O$ was dissolved in each DES, following by uniformly stirring. This mixed liquid was then heated at 150 °C for 15 h without stirring under atmospheric pressure in an air environment, resulting in the formation of black precipitants. After cooling, the precipitants were centrifuged and washed with distilled water and absolute ethanol. Final products were obtained by drying precipitants at 60 °C under vacuum overnight. For further synthesis, Bi_2S_3 was synthesized by varying the amount of TAA in the TAA/acetamide-based DES, maintaining a TAA concentration of 2-40 mol% relative to acetamide.

Material Characterization. The crystalline phases were determined by X-ray diffraction (XRD) method using X-ray diffractometer (D2 PHEASER with Cu-Kα radiation (λ=1.54059 Å), Bruker) at a voltage of 30 kV and a current of 10 mA. Functional groups were analyzed by FTIR technique using Fourier Transform Infrared Spectrometer (FT/IR-660D-ATR, JASCO. Co.) in the range of 400–4000 cm^{-1}. Particle morphologies were observed by using scanning electron

microscope (SEM, SU6600, Hitachi High-Tech Co.) at an acceleration voltage of 10 kV, and transmission electron microscope (TEM, JEM-2100Plus, JEOL Ltd.) at an acceleration voltage of 200 kV. The diffuse reflectance (DR) spectra were recorded using a UV-visible-NIR spectrophotometer (V-670, JASCO Co.) attached with an integrated sphere and the optical band gaps were estimated by Kubelka-Munk transformed DR spectra, specifically using Tauc plot. Thermal stabilities were assessed through thermal gravimetric and differential thermal analyses (TG-DTA) in an air atmosphere at heating rate of 10 °C/min, measured by using a Thermogravimetric Differential Thermal Analyzer (Thermo plus EVO2, Rigaku CO.).

Gas sensing measurement. Gas sensers were fabricated by a drop-casting procedure. First, 10 μg of Bi_2S_3 powder samples were dispersed in 20 μL of absolute ethanol and sonicated to form a suspension. The gas sensing electrodes were placed on the hot plate at 75 °C, and suspension were added dropwise onto the electrodes. The electrodes were prepared using the EMD-4000B purchased from Amphenol Advanced Sensors Inc., USA, after removing the surface coating with acetone. Afterward, the electrodes were dried at 60 °C. Characterization was performed in a lab-made gas-flow measurement chamber, and the instantaneous resistance values were recorded using an ultrahigh resistance meter (5451, ADCMT Co.). All measurements were carried out at 50 °C to accelerate the response, with temperature was controlled by thermocouple. During the measurement, a constant voltage of 10 V was applied. The gas chamber Measurements were filled with dried air, allowing the resistance to stabilize before measurements. The concentrations of the target gas were adjusted by varying the flow rate ratio of dried air to target gases, while maintaining a total gas flow of 200 mL/min. The gas sensors were exposed to specific concentrations of the target gas for 15 minutes, followed by exposure to only dried air for 15 minutes to recover the resistance values. This cycle was repeated with increasing concentrations of the target gas, and changes in resistance values were recorded.

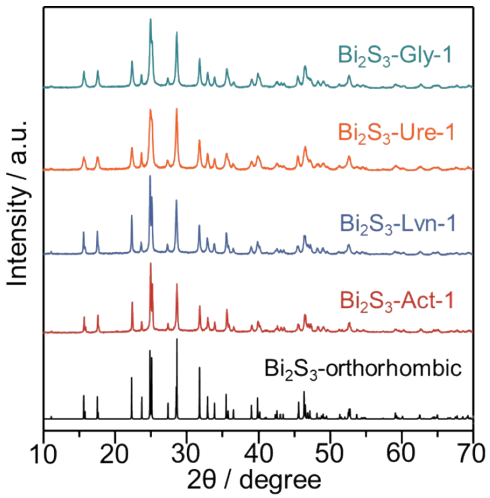

Figure S1 XRD patterns of Bi_2S_3 synthesized using various DESs.

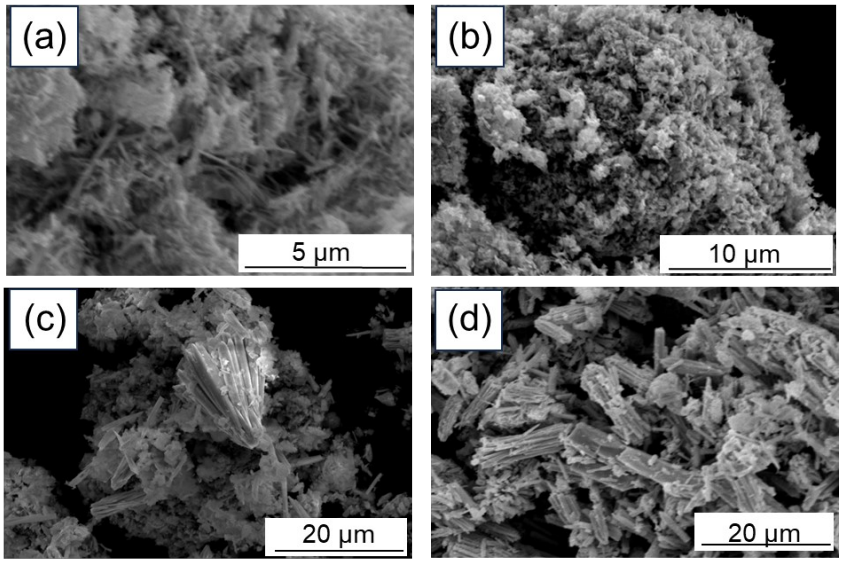

Figure S2. SEM images of (a) Bi_2S_3-Gly-1, (b) Bi_2S_3-Ure-1, (c) Bi_2S_3-Lvn-1, (d) Bi_2S_3-Act-1

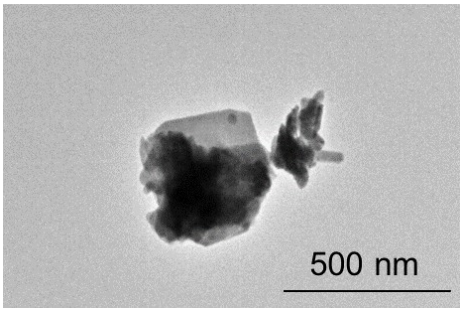

Figure S3 TEM image of Bi_2S_3-Ure-1.

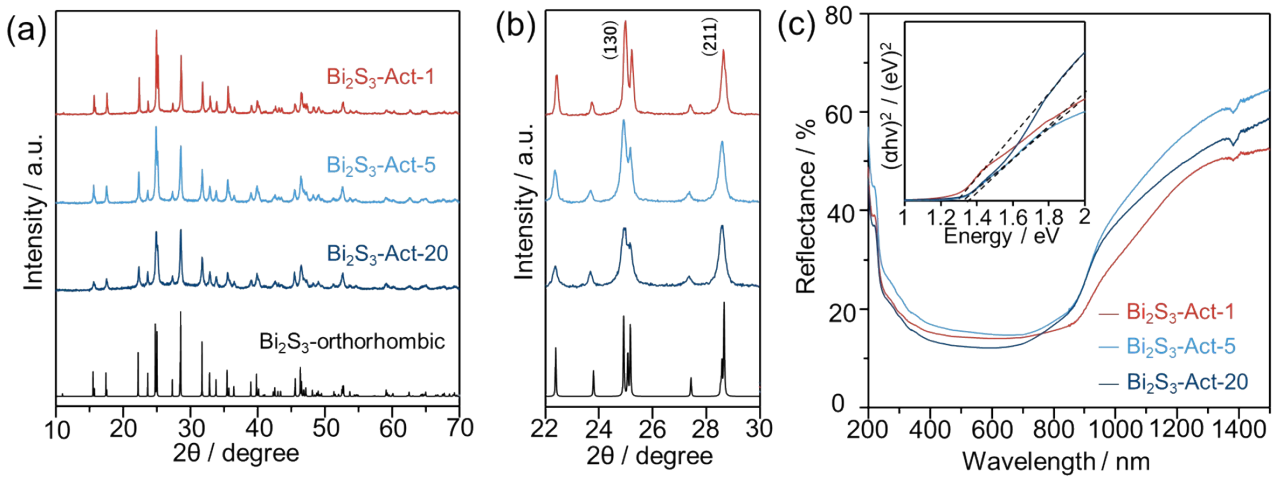

Figure S4 (a) XRD patterns in the range of 10–70 degree, (b) XRD patterns in the range of 22–30 degree, (c) UV-vis-NIR reflectance diffuse spectra of Bi_2S_3 synthesized using different amount of TAA. The inset in (c) displays the Tauc plot, the intersection of the dotted black line and the x-axis indicates the direct band gap.

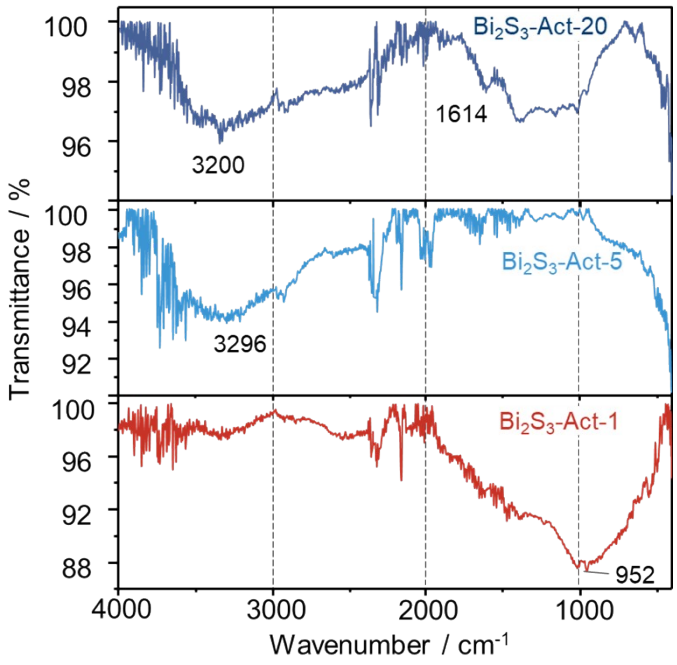

Figure S5 FTIR spectra of Bi_2S_3 synthesized using different amount of TAA in DESs.

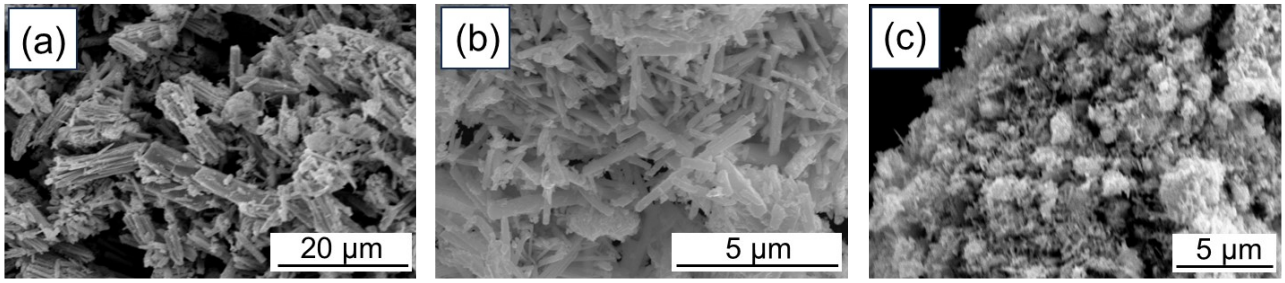

Figure S6 SEM images of (a) Bi_2S_3-Act-1, (b) Bi_2S_3-Act-5, (c) Bi_2S_3-Act-20.

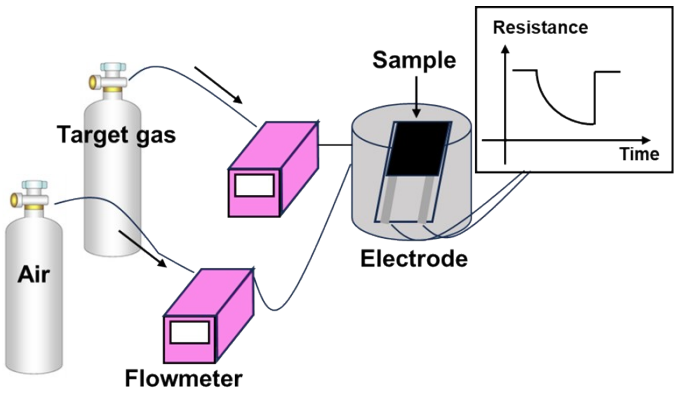

Figure S7 Schematic illustration of gas sensing system.

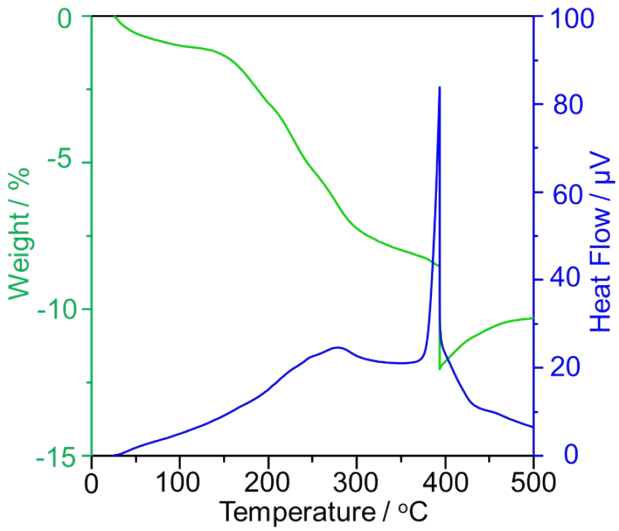

Figure S8 TG-DTA curve of Bi_2S_3-Act-20 Sharp mass decrease at 400 °C occurred because of decomposition of Bi_2S_3.

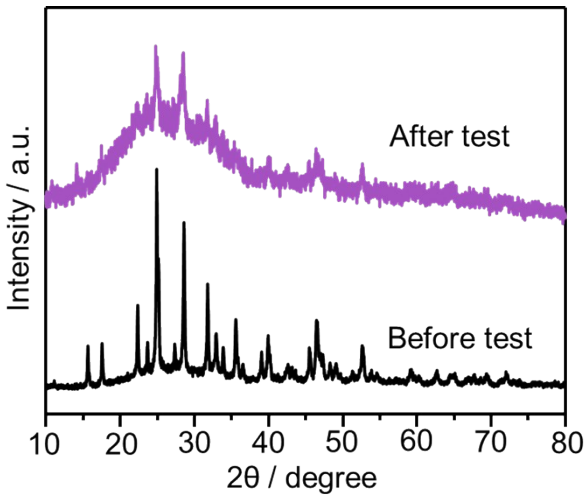

Figure S9 Comparison of XRD patterns of Bi_2S_3-Act-20 before and after test.

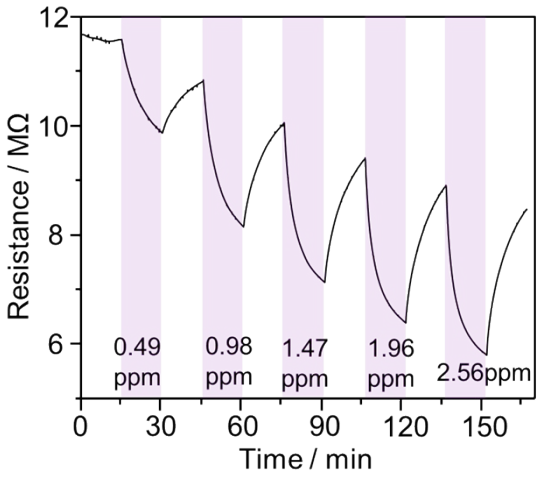

Figure S10 Dynamic resistance variation of Bi_2S_3-Act-20 gas sensor towards H_2S gas.

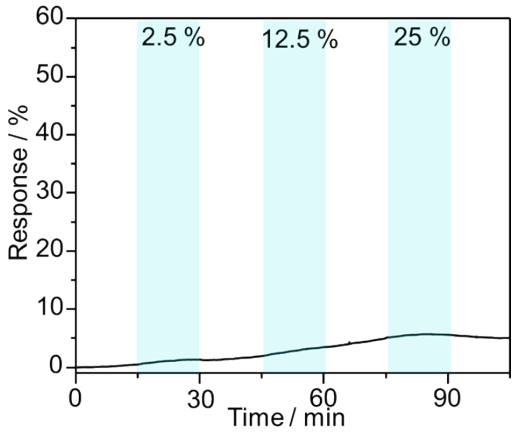

Figure S11 Response variation of Bi_2S_3-Act-20 gas sensor to humidity air. The values displayed above the figure represent the relative humidity at 50 ℃.

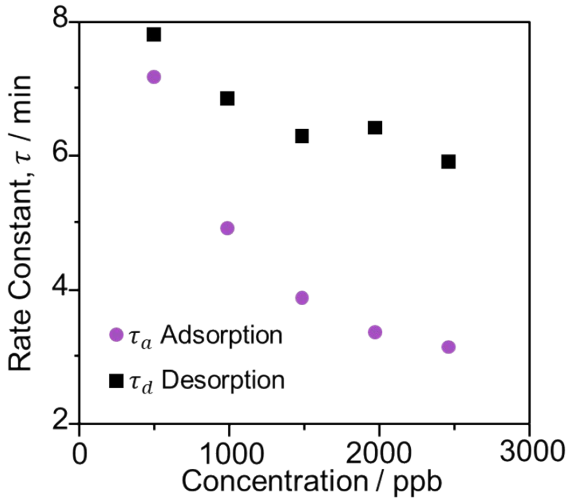

Figure S12 Adsorption/desorption rate consistent (τ) vs. H_2S gas concentration.

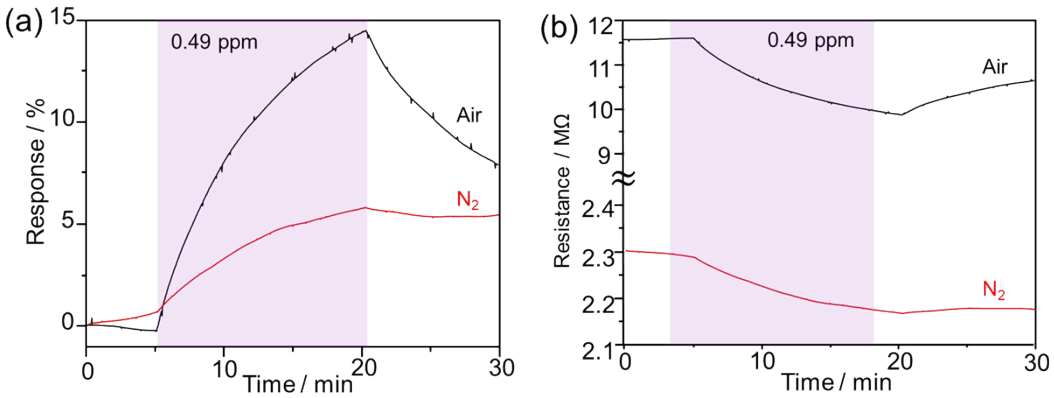

Figure S13Comparison of (a) response and (b) resistance with different background gases.

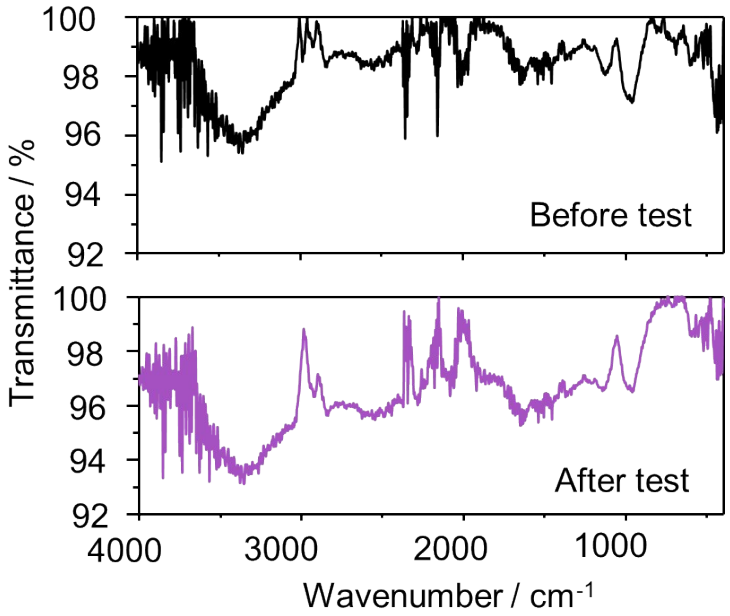

Figure S14 Comparison of FTIR spectra of Bi_2S_3-Act-20 before and after test.

Table S1 Response/recovery times of Bi_2S_3-Act-20 gas sensor to H_2S gas for each concentration.

Concentration / ppb	Response time / min	Recovering time / min
0.491	16.5	18
0.982	11.3	15.8
1.47	8.9	14.5
1.96	7.7	14.7
2.46	7.2	13.6